

AD-A149 443

MODELING AND SIMULATION OF A FIN ACTUATION SYSTEM(U)
NAVAL POSTGRADUATE SCHOOL MONTEREY CA R H NUNN ET AL.
DEC 84 NPS69-84-011

1/1

UNCLASSIFIED

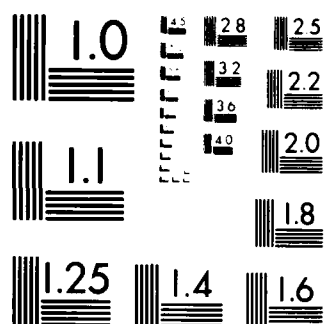
F/G 16/4

NL

END

FILMED

071C



MICROCOPY RESOLUTION TEST CHART
NATIONAL BUREAU OF STANDARDS 1963-A

2

NPS69-84-011

NAVAL POSTGRADUATE SCHOOL

Monterey, California

AD-A149 443



DTIC
ELECTE
JAN 24 1985
B

Modeling and Simulation of a
Fin *ACTUATION* System

R. H. Nunn
R. J. Wright

December 1984

Progress report for period
October, 1983 - September, 1984

Approved for Public Release; Distribution Unlimited

Prepared for: Naval Weapons Center, Code 3275
China Lake, California 93555

85 01 11 003

NAVAL POSTGRADUATE SCHOOL
Monterey, California

Commodore R. H Shumaker
Superintendent

D. A. Shradly
Provost

The work reported herein was supported by the Naval Weapons Center, Code 3275,
China Lake, California 93555.

Reproduction of all or part of this report is authorized. This report was
prepared by:



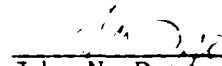
Robert H. Nunn
Professor of Mechanical Engineering

Reviewed by:

Released by:



Paul J. Merto
Chairman, Department of
Mechanical Engineering



John N. Dyer
Dean of Science and Engineering

Unclassified

SECURITY CLASSIFICATION OF THIS PAGE (When Data Entered)

REPORT DOCUMENTATION PAGE		READ INSTRUCTIONS BEFORE COMPLETING FORM
1. REPORT NUMBER NPS69-84-011	2. GOVT ACCESSION NO. AD-A149443	3. RECIPIENT'S CATALOG NUMBER
4. TITLE (and Subtitle) Modeling and Simulation of a Fin Actuation System	5. TYPE OF REPORT & PERIOD COVERED Progress Report Oct 83 - Sep 84	
	6. PERFORMING ORG. REPORT NUMBER NPS69-84-011	
7. AUTHOR(s) R. H. Nunn R. J. Wright	8. CONTRACT OR GRANT NUMBER(s)	
9. PERFORMING ORGANIZATION NAME AND ADDRESS Naval Postgraduate School Monterey, CA 93943	10. PROGRAM ELEMENT, PROJECT, TASK AREA & WORK UNIT NUMBERS	
11. CONTROLLING OFFICE NAME AND ADDRESS Naval Weapons Center, Code 3275 China Lake, CA 93555	12. REPORT DATE December 1984	
	13. NUMBER OF PAGES 30	
14. MONITORING AGENCY NAME & ADDRESS (if different from Controlling Office)	15. SECURITY CLASS. (of this report) Unclassified	
	15a. DECLASSIFICATION/DOWNGRADING SCHEDULE	
16. DISTRIBUTION STATEMENT (of this Report) Approved for public release; distribution unlimited		
17. DISTRIBUTION STATEMENT (of the abstract entered in Block 20, if different from Report)		
18. SUPPLEMENTARY NOTES		
19. KEY WORDS (Continue on reverse side if necessary and identify by block number) electromechanical, modeling, simulation		
20. ABSTRACT (Continue on reverse side if necessary and identify by block number) A study was begun to model and simulate a missile fin actuation system driven by a brushless dc motor. This report describes preliminary results in which the motor, drive-train and load were modeled using the usual linear descriptions. Simulation of system response to step and frequency inputs was accomplished using the Continuous System Modeling Program. Initial qualitative results show that the model successfully predicts the effects expected from variations in load and damping. Further evaluation of the model and possible refinements will require the availability of test data.		

DD FORM 1473
1 JAN 73EDITION OF 1 NOV 68 IS OBSOLETE
S N 0102-LF-014-6601

Unclassified

SECURITY CLASSIFICATION OF THIS PAGE (When Data Entered)

MODELING AND SIMULATION OF A FIN ACTUATION SYSTEM

SUMMARY

A study was begun to model and simulate a missile fin actuation system driven by a brushless dc motor. This report describes preliminary results in which the motor, drive-train, and load were modeled using the usual linear descriptions. Simulation of system response to step and frequency inputs was accomplished using the Continuous System Modeling Program.

Initial qualitative results show that the model successfully predicts the effects expected from variations in load and damping. Further evaluation of the model and possible refinements will require the availability of test data.

TABLE OF CONTENTS

List of Symbols	vi
Introduction	1
Theory and Analysis	3
Motor Analysis	6
Preliminary Results and Conclusions	6
List of References	15
Appendices	
Initial Distribution List	

Accession For		<input checked="checked" type="checkbox"/>
NTIS GRA&I		<input type="checkbox"/>
DTIC TAB		<input type="checkbox"/>
Unannounced		<input type="checkbox"/>
Justification		
PER CALL JC		
By		
Distribution/		
Availability Codes		
Dist	Avail and/or Special	
A-1		



LIST OF SYMBOLS

R_m	Coefficient of viscous friction of the motor (rad/sec)
E_a	Control input voltage
E_b	Generated voltage (back emf)
F_s	Force acting on the ball screw
I_s	Stator current
J_c	Moment of inertia of the crank
J_m	Moment of inertia of motor shaft
J_{s2}	Moment of inertia of output shaft
K_b	Back emf constant
K_i	Torque constant
L	Lead of ball screw
L_s	Inductance of the stator windings
M_h	Fin hinge moment
M_s	Mass of the ball screw
N	Gear ratio
P	Pitch
R_s	Resistance of 2 stator windings
T_f	Sum of the friction forces acting on the actuator
T_m	Torque generated by the motor
T_L	Torque acting on the motor output shaft
X	Linear displacement of the ball screw
θ_m	Angular displacement of the motor shaft
θ_o	Angular displacement of the fin

INTRODUCTION

Recent improvements in rare-earth magnetic materials for use in brushless dc motors have allowed reconsideration of electro-mechanical actuator systems for applications requiring very high ratios of torque-to-inertia. The investigation discussed herein has been concerned with characterizing mathematically the dynamical features of a missile fin actuation system, from the input to the brushless dc motor to the output shaft of the mechanical actuator. The physical model is based upon an existing prototype actuator currently under evaluation at the Naval Weapons Center, China Lake, California.

In general, brushless dc motors produce torque through the interaction of a magnetic field generated by a permanent magnet rotor and a dc generated magnetic field in the stator. The rotating permanent magnet eliminates the rotating armature and the mechanical wear normally associated with brushes. These motors fall in the class of Permanent Magnet Motors and enjoy certain advantages over wound-field types such as:

"...linear torque-speed characteristics, high stall (accelerating) torque, no need for electric power to generate the magnetic flux and a smaller frame and lighter motor for a given output power" [1].

Additionally, the brushless dc motor is characterized by:

"...controllability over a wide range of speeds, capable of rapid acceleration and deceleration, convenient control of shaft speed and position, no mechanical wear problem due to commutation and better heat dissipation arrangement" [1].

The fundamental requirement of an electro-mechanical actuator control system is to provide torque to an output shaft, sense the position of the shaft and adjust the torque to balance the load when the desired position is reached. This must be accomplished with a minimum of frictional resistance and delays associated with the inertia of the mechanical components. Effects of viscous, static and coulomb friction, together with the torque required to

accelerate the mechanical components of the system, lead to a reduction in torque available at the output shaft and an associated reduction in system performance.

One approach to the analysis of the electro-mechanical actuator system has been to divide the system into two sequential problem areas. The first deals with the dynamic analysis of the brushless dc motor and development of the transfer function necessary to duplicate actual steady-state and transient performance. The second area deals with modeling the mechanical system elements, taking as input the dc motor shaft angular acceleration predicted by the motor analysis. The mechanical system must be modeled considering the effects of friction and inertia and translating the rotational motion of the brushless dc motor shaft to the output shaft of the actuator for application to missile maneuvering control. This report documents the results obtained from a study that has placed primary emphasis upon the latter problem area - the modeling of the mechanical drive-train leading to the fin shaft [2]. The influences of various design aspects of brushless dc motors are not given detailed attention here, but such matters have been studied in parallel investigations [3, 4].

The remainder of this report presents the results of attempts to formulate a mathematical model of a brushless dc motor and a mechanical actuator as might be installed on a Navy tactical missile. The model has been implemented in a computer program so that parametric studies may be conducted to determine output characteristics (torque, speed, acceleration) as functions of input forms and design options. Additionally, the modular format used in CSMP¹ will facilitate incorporation of future technology and allow inputs for use in both design and analysis.

¹ The Continuous System Modeling Program (CSMP) is a program especially developed by IBM to allow users to simulate physical systems with a minimum of programming difficulty. Details are provided, for instance, in Ref. 5.

THEORY AND ANALYSIS

GENERAL

The system is viewed as a position control device to maintain an output angle under an applied hinge moment due to aerodynamic forces on a fin or aileron. The motor is a permanent magnet dc motor with feedback in the form of back emf proportional to the angular velocity of the motor. The block diagram of the dc motor is shown in Fig. 1 [6]. The mechanical actuator and drive train, as currently envisioned, introduce various inertial and damping loads together with an aerodynamic force and its associated fin hinge moment that must be overcome to produce output motion. An operational block diagram of the load torque is shown in Fig. 2 where the hinge moment and motor shaft angular acceleration are viewed as inputs to the drive train. Figure 3 is a schematic of the drive train which, as presently constituted, includes the motor shaft (leadscrew), ball screw assembly, and the crank which is keyed to the output (fin) shaft. Inertial loads are considered individually within three major subdivisions of the actuator; the output shaft to crank, crank to ball screw, and ball screw to leadscrew.

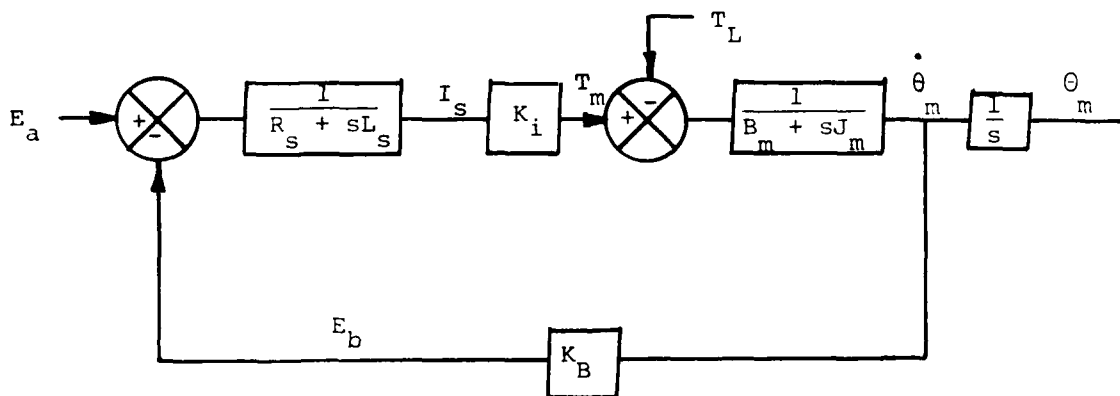


Figure 1. Standardized Block Diagram of a DC Motor

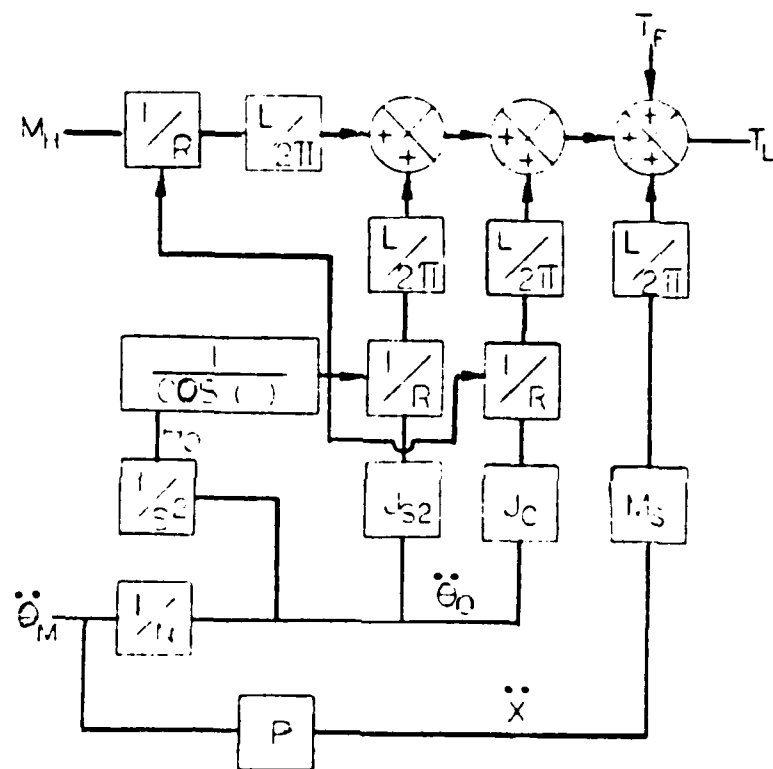


Figure 2. Operational Block Diagram of the Load Torque

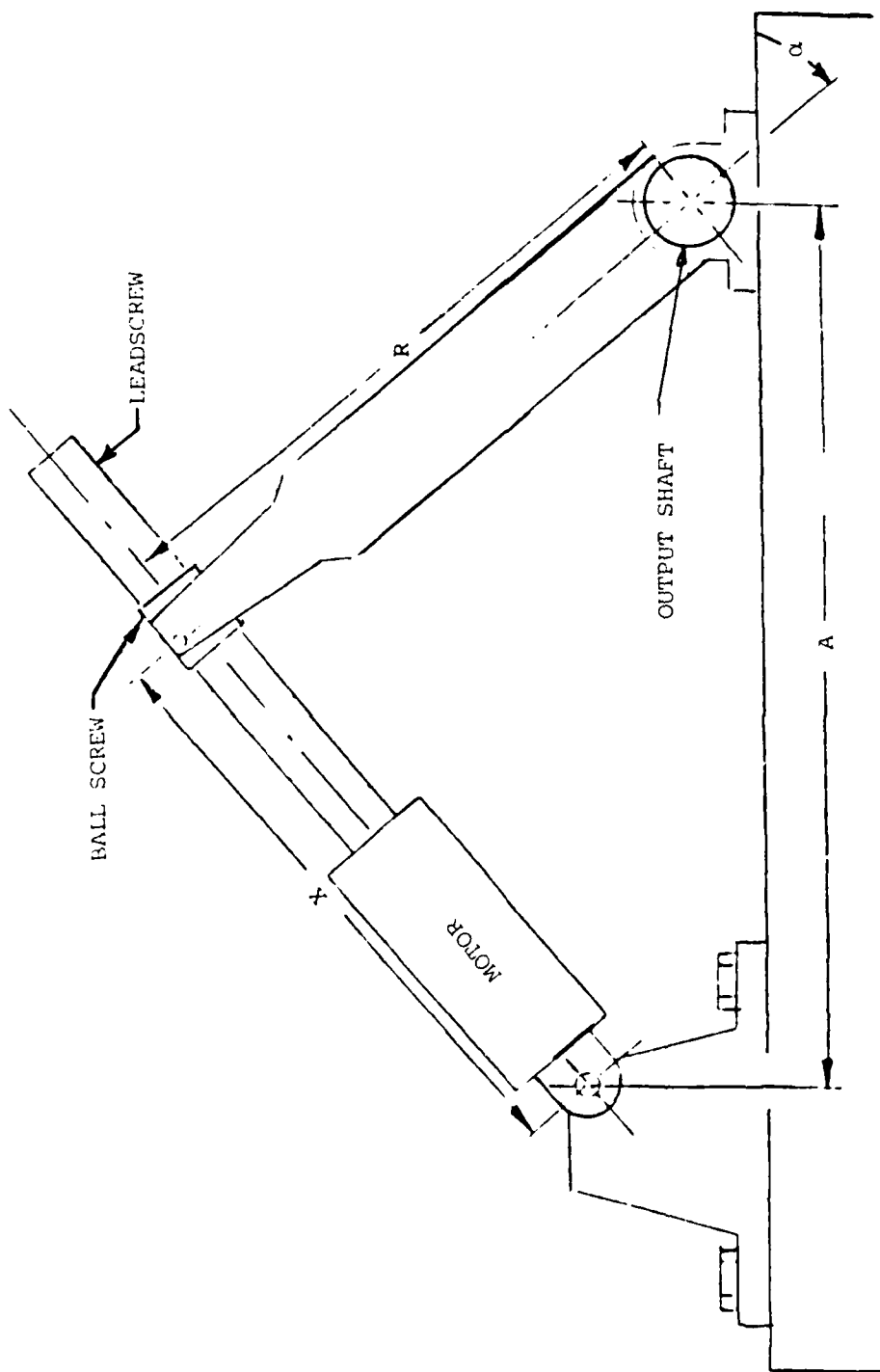


Figure 3. Schematic of the Drive Train

MOTOR ANALYSIS

The voltage drop across the stator windings of a permanent magnet brushless dc motor may be written

$$E_a - E_b = L_s \frac{dI_s}{dt} + R_s I_s \quad (1)$$

and the current leads to a developed torque given by

$$T_m = K_i I_s \quad (2)$$

This torque must overcome frictional loads and inertias reflected to the motor output shaft while at the same time supplying a demanded load torque T_L so that

$$T_m = J_m \ddot{\theta}_m + B_m \dot{\theta}_m + T_L \quad (3)$$

(In the simple model developed herein we have assumed that spring loads due to elasticity in the drive train are negligible.) The back emf is approximated as proportional to the motor speed (the electrical counterpart of viscous friction) with the result that

$$E_b = K_b \dot{\theta}_m \quad (4)$$

Equations (1) - (4) may be viewed as governing the time variation of the variables E_b , I_s , T_m , and θ_m in response to input voltage E_a and constrained by the load torque T_L . The internal motor parameters are L_s , R_s , K_i , and K_b , while the mechanical features of the motor are characterized by J_m and B_m . The various functional relationships are illustrated in Fig. 1.

LOAD ANALYSIS

The power transmission system is illustrated in Fig. 3 and contains a ball screw that converts the axial component, F_s , of the force required by the load

on the ball screw into a load torque T_L acting on the motor shaft (leadscrew). The conversion is given by

$$T_L = (F_S L) / 2\pi \quad (5)$$

where L is the lead (distance the ball screw moves parallel to the axis of the leadscrew for one revolution of the leadscrew). This relationship, the development of which is discussed further in Ref. 2, requires the assumption of negligible frictional effects in the ball screw. The force transmitted as torque through the action of the ball screw is parallel to the axis of the leadscrew only when the crank is orthogonal to the leadscrew. As a result, a nonlinear relationship exists between the force acting on the ball screw and the torque reflected back through the system from the output shaft (see Appendix A).

Pitch P is the ratio of the linear displacement X of the ball screw to the angular displacement ϕ_m of the motor shaft. The gear ratio N is defined here as the ratio of the angular displacement of the motor shaft to the angular displacement ϕ_o of the output shaft. The relationship between pitch and gear ratio, for a given drive train geometry, is also developed in Appendix A.

The sum F_S of the load forces acting on the ball screw depends upon the fin hinge moment M_h due to the aerodynamic forces acting on the aileron, the moment of inertia of the output shaft J_{S2} , the moment of inertia of the crank J_C , the angular acceleration $\ddot{\phi}_o$ of the output shaft (assumed to be the same as the crank, i.e., the output shaft is of infinite stiffness), and the mass M_S and linear acceleration \ddot{X} of the ball screw.

$$F_S = M_S \ddot{X} + [(J_C \ddot{\phi}_o + J_{S2} \ddot{\phi}_o + M_h) / (R \cos \phi_o)] \quad (6)$$

Combining with Eq. (5), along with the addition of the (unknown) frictional forces T_f acting on the actuator, allows the load torque T_L to be expressed as a function of the axial acceleration of the ball screw \ddot{X} and the angular acceleration of the motor $\ddot{\theta}_m$.

$$T_L = \frac{L}{2\pi} \left[M_s \ddot{X} + \frac{\ddot{\theta}_m (J_c + J_{s2})}{R \cos(\theta_m/N)} + M_h \right] + T_f \quad (7)$$

A number of additional relationships may be developed by means of various combinations of the preceding equations. For example, Eqs. (1) through (4) may be combined to yield the transfer function for the torque motor:

$$\frac{\dot{\theta}_m}{E_a} = \frac{K_i - \frac{T_L}{I_s}}{(L_s s + R_s) (J_m s + B_m) + K_b (K_i - \frac{T_L}{I_s})} \quad (8)$$

This expression is useful for simply-described (e.g., zero) load torques T_L . Equation (8) may be combined with Eq. (7) and the gear ratio N to obtain the actuator output response ($\dot{\theta}_o = \dot{\theta}_m/N$) to input voltage E_a .

The CSMP code used to solve these governing equations is given in Appendix B, together with a summary of the logic flow.

PRELIMINARY RESULTS AND CONCLUSIONS

Validation in mathematical modeling requires a comparison between response predictions obtained through simulation and data produced as a result of experiments. At this writing, test data have not become available for the electro-mechanical actuator modeled in this study and, therefore, the precision of the model's representation of reality remains untested. For the present, therefore, the "credibility" of the model must be based on the reasonableness of the model's dependency upon certain key variables such as the viscous friction of the motor and the level of the applied load.

Figure 4 shows the predicted response to a 30-volt step input under zero applied load using the manufacturer's specifications¹ for the viscous friction of the motor. For comparison, a 90-percent reduction in the viscous friction of the motor under the same input and load conditions produces the slightly underdamped response shown in Fig. 4. A decrease in the viscous friction of the motor produces the expected change in the output response, but the system remains highly stable due to the back-emf effect in the motor.

For further comparison, Figs. 5 through 7 were obtained using a 30-volt step input and manufacturer's specification for the viscous friction of the motor. Figure 5 depicts the fin angle versus time for this nominally-damped system under varying loads. As expected, the fin angle produced for a given time decreases with an increase in the output load. This is in agreement with Fig. 6 where the steady-state fin rate is seen to decrease with an increased load. The steady state rate response for the zero load condition, obtained from Eq. (8), is given by

¹ Numerical values used to define the nominal design are listed in Appendix B, Figure B1.

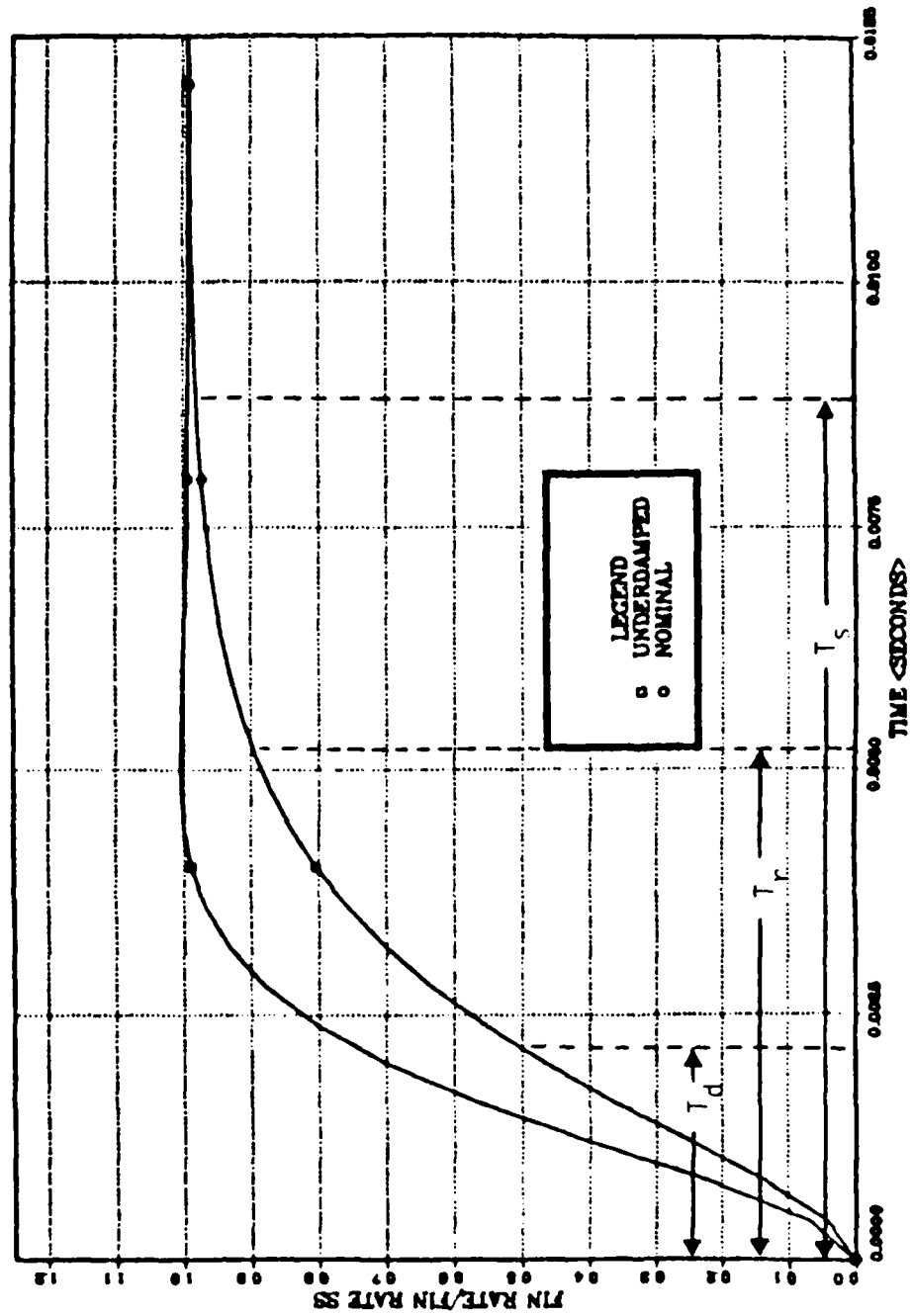


Figure 4. Fin Rate Response to Step Input; Nominal and Underdamped.

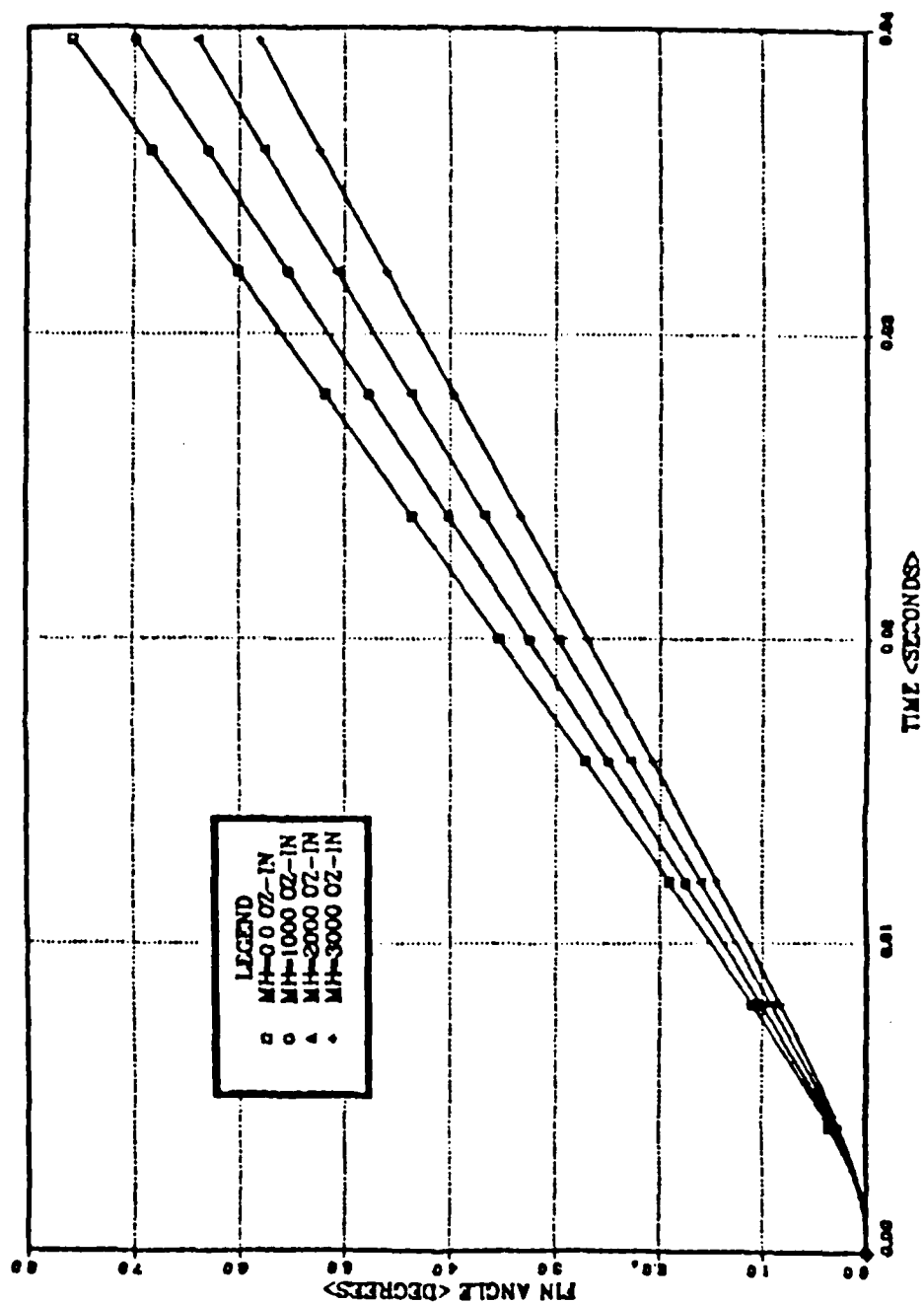


Figure 5. Fin Angle Response to Step Input; Various Hinge Moments.

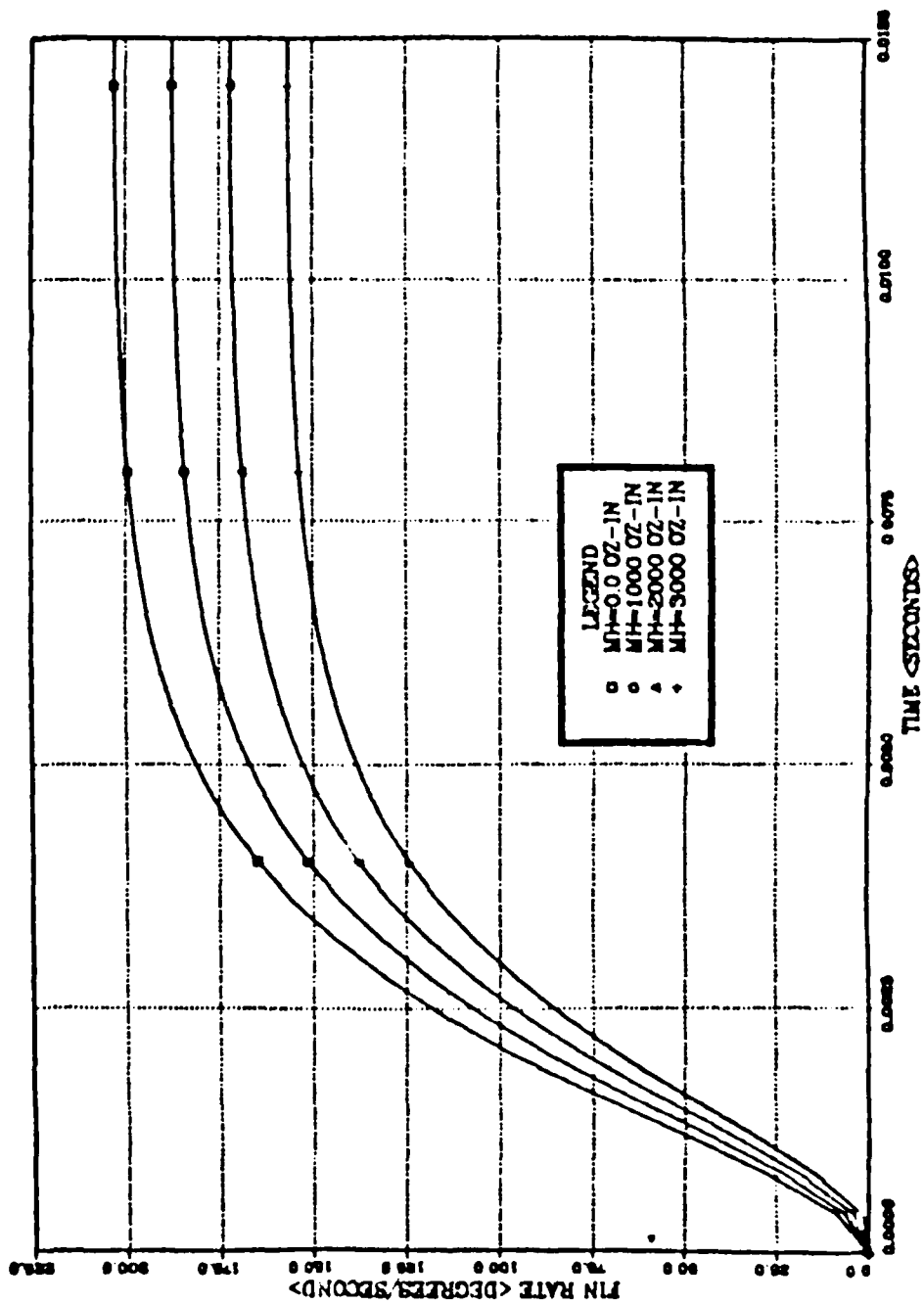


Figure 6. Fin Rate Response to Step Input; Various Hinge Moments.

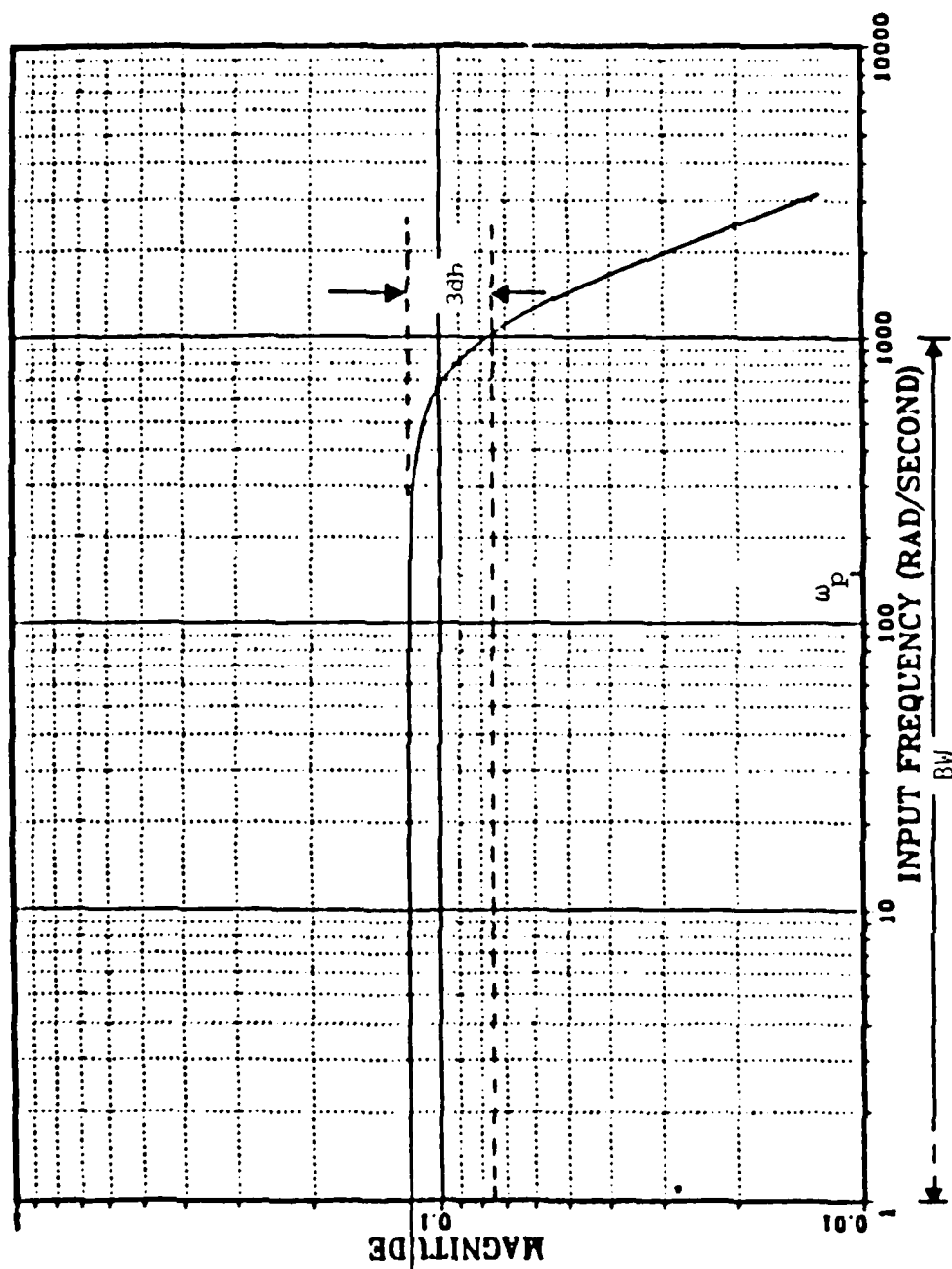


Figure 7. Frequency Response; Nominal Damping, No Load.

$$\dot{C}_O = K_i E_a / [N(R_S R_m + K_i K_b)] \text{ (steady state)} \quad (9)$$

and for the nominal case studied here a value of 203.3 degrees/second is obtained, as indicated in the no-load curve of Fig. 6. The frequency response results shown in Fig. 7 were obtained using zero applied load and nominal design conditions. The nominal second-order system response in Fig. 4 illustrates reasonable time-domain specifications for delay time ($T_d = 0.0020$ seconds), rise time ($T_r = 0.0055$ seconds) and settling time ($T_s = 0.0090$ seconds). Corresponding frequency response characteristics, illustrated in Fig. 7, are bandwidth ($BW = 159$ Hz), cutoff frequency ($\omega_c = 159$ Hz) and resonant frequency ($\omega_p = 28$ Hz).

The program currently models a second order open-loop system providing an output velocity dependent upon an input voltage. Two considerations were deliberately neglected in order to simplify the initial model construction, mechanical backlash between the leadscrew and ball screw and torsional deflection in the output shaft. Inclusion of both within the NOSORT section of the CSMP code would bring the model in closer alignment with the physical system. In addition, incorporation of angular position control in the form of position feedback added as a macro to the original code would increase the program utility. Determination of the extent to which these and other refinements are necessary must await the availability of test data.

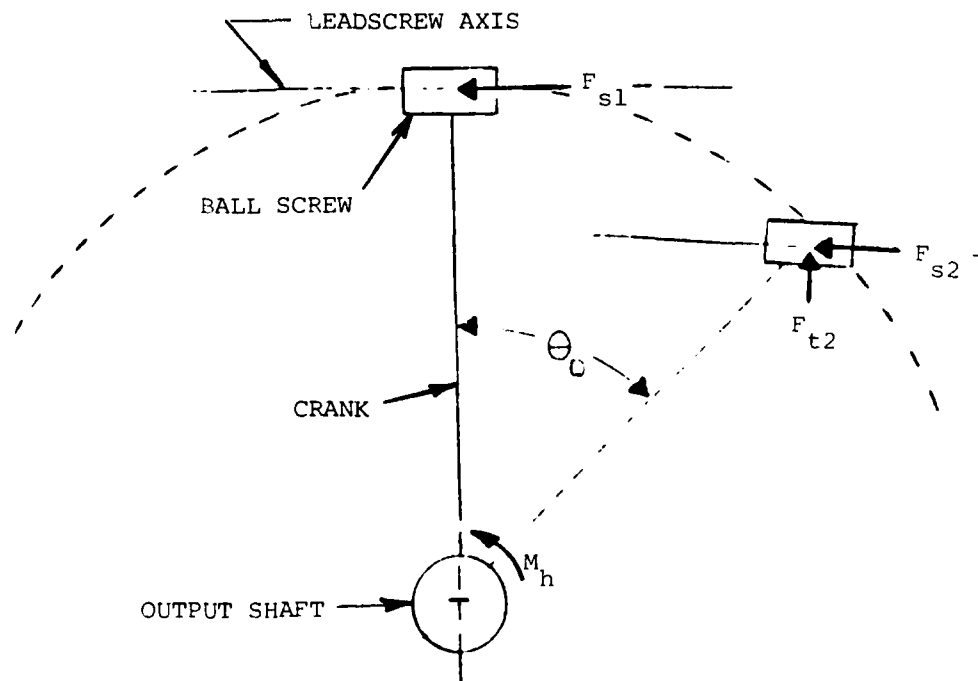
LIST OF REFERENCES

1. Electro-Craft Corporation, DC Motors, Speed Controls, Servo-Systems, an Engineering Handbook, Electro-Craft Corporation, 1980.
2. Wright, R. J., "Simulation and Synthesis of Electro-Mechanical Actuators," M.S. Thesis, Department of Mechanical Engineering, Naval Postgraduate School, Monterey, CA, September, 1984.
3. Thomas, S. M., "CSMP Modeling of Brushless DC Motors," M.S. Thesis, Department of Electrical and Computer Engineering, Naval Postgraduate School, Monterey, CA, September, 1984.
4. Askinas, A., "Pulse Width Modulated Speed Control of Brushless DC Motors," M.S. Thesis, Department of Electrical and Computer Engineering, Naval Postgraduate School, Monterey, CA, September, 1984.
5. Speckhart, F. H. and Green, W. L., A Guide to Using CSMP-The Continuous System Modeling Program, Prentice-Hall, NJ, 1976.
6. Kuo, B. C., Automatic Control Systems, Prentice-Hall, Inc., 1982.
7. Shigley, J. E. and Mitchell, L. D., Mechanical Engineering Design, McGraw-Hill Book Company, 1983.

APPENDIX A

CRANK/BALL SCREW TRANSFER

The physical arrangement of the leadscrew, ball screw, crank and output shaft is illustrated in Fig. 3. The output load which appears as a torque M_h on the output shaft, is transmitted as a force acting with the moment arm created by the crank. When the crank is orthogonal to the leadscrew, the force acting on the ball screw as a result of the output load is parallel to the axis of the leadscrew and is transmitted to the leadscrew as shown in the sketch below. However, in order to affect output shaft rotation, the crank is



generally not orthogonal to the leadscrew and the force vector acting on the ball screw is no longer parallel to the axis of the leadscrew. The force vector acting on the ball screw is represented as an axial force F_s and a transverse force F_t in the sketch. The axial force may be written as

$$F_s = M_h / (R \cos \theta_o)$$

where R is the length of the crank measured from the axis of the output shaft to the axis of the leadscrew and θ_o is the output shaft orientation measured such that θ_o is zero when the two axes are perpendicular. The result effectively shortens the moment arm generated by the crank and increases the axial force acting on the ballscrew for a given output load.

GEAR RATIO

The gear ratio N is defined as the ratio of the angle θ_m turned by the motor shaft to the angle θ_o turned by the output shaft. In differential form,

$$N = d\theta_m / d\theta_o$$

and, in terms of ball screw displacement X ,

$$N = (d\theta_m / dX) (dX / d\theta_o)$$

The first term in this expression is the reciprocal of the pitch of the ball screw and the second term is related to the geometry of the drive train following the ball screw.

The geometry illustrated in Fig. 3 leads to the relationship

$$X^2 = A^2 + R^2 - 2AR \cos \alpha \tag{A1}$$

where α is the orientation of the crank arm measured relative to a fixed reference frame. Taking the derivative of this expression with respect to α

$$dX / d\alpha = AR \sin \alpha / X$$

and after elimination of $\sin \alpha$ by means of Eq. (A1)

$$dX/d\alpha = [(2AR)^2 - (A^2 + R^2 - X^2)^2]^{1/2} / 2X \quad (A2)$$

This expression has a maximum at $X = X_{\text{ref}} = (A^2 - R^2)^{1/2}$ which corresponds to the configuration when the output crank and motor shaft are perpendicular, that is, when $\theta_0 = 0$. For the design presently under consideration, $A = 6.875$ in. and $R = 1.887$ in. so that $X_{\text{ref}} = 6.6110$ in. The corresponding value of α is $\alpha_{\text{ref}} = \tan^{-1} (X_{\text{ref}}/R) = 74.07$ degrees. For any given design this is a fixed value such that $\alpha = \alpha_{\text{ref}} + \theta_0$ and $dX/d\alpha = dX/d\theta_0$. The gear ratio is $N = (dX/d\theta_0)/P$ so that with Eq. (A2):

$$N = [(2AR)^2 - (A^2 + R^2 - X^2)^2]^{1/2} / 2XP$$

The maximum value of N occurs at $X = X_{\text{ref}}$ and is given by $N_{\text{max}} = R/P$, (74.1 for the present design).

Figure A1 shows the variation of the gear ratio around the maximum value in terms of ball screw position X and Fig. A2 illustrates the effect of the nonlinearity for the present design over a range of fin deflections. Operation of the actuator within 90 percent of the maximum gear ratio would allow a fin deflection of about 25 degrees relative to θ_0 .

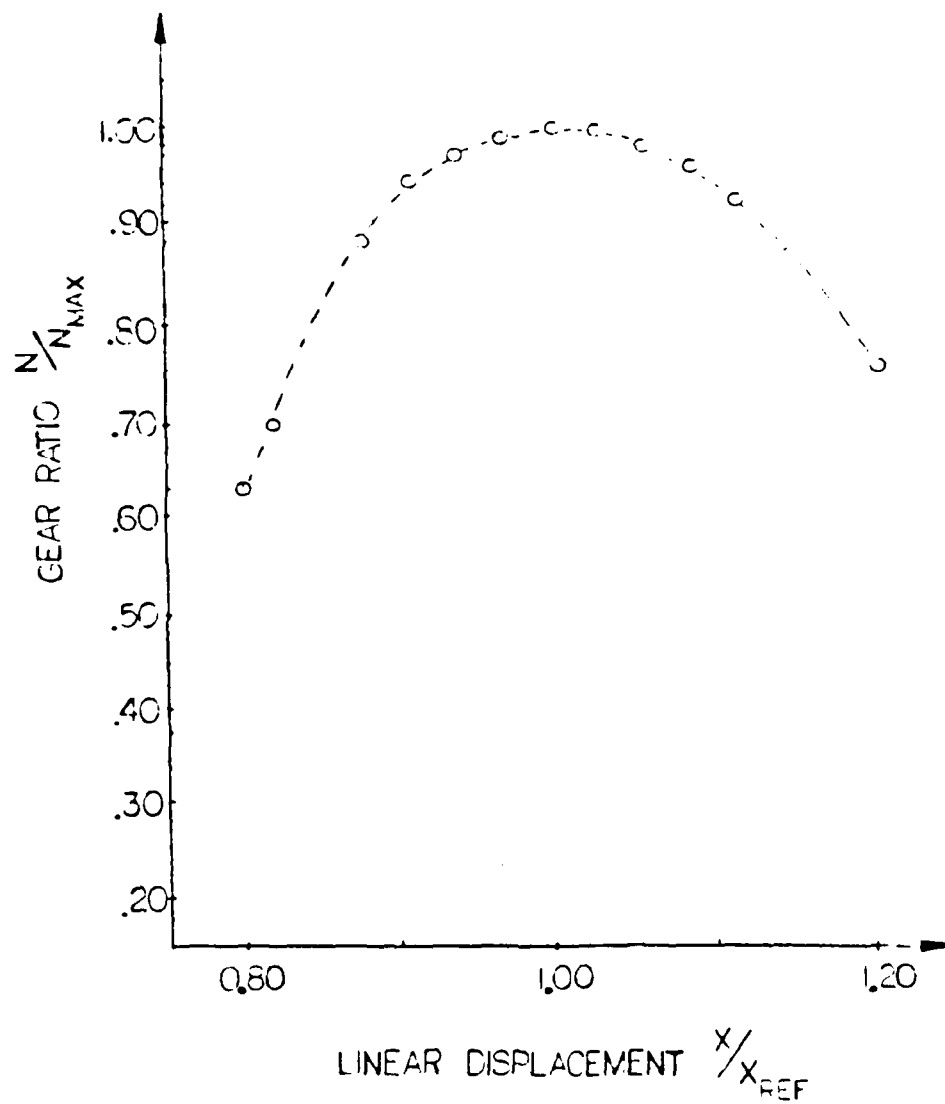


Figure A1. . Ball Sleeve Travel vs. Gear Ratio.

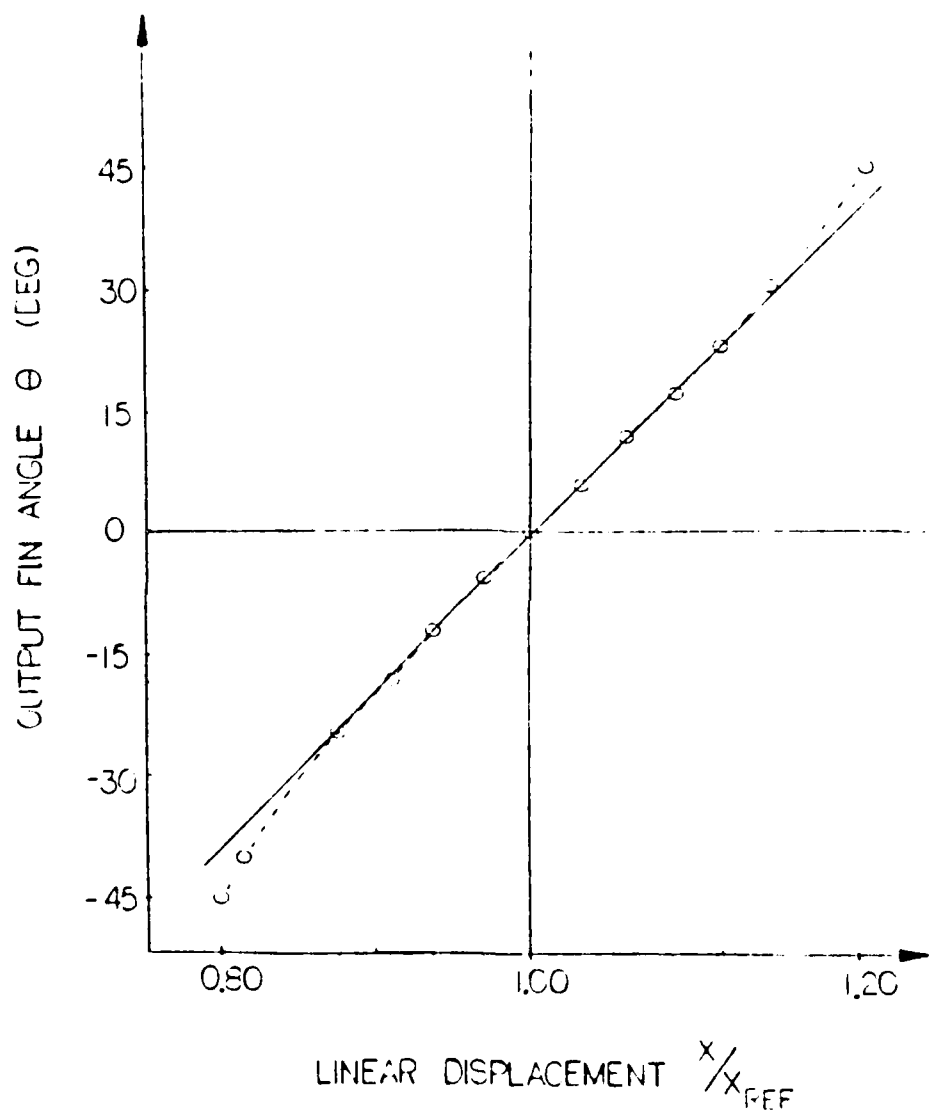
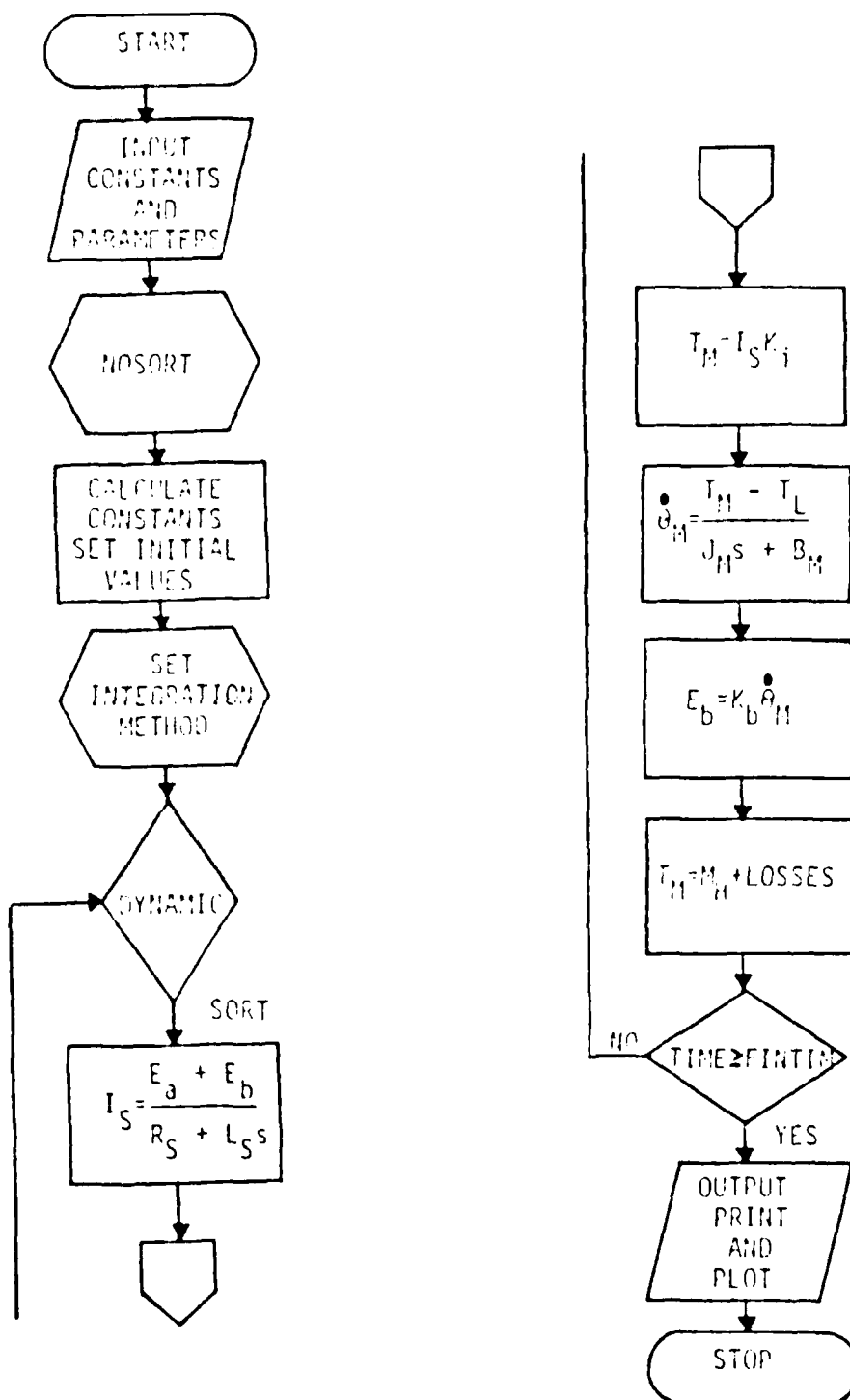


Figure A2. Fin Angle vs. Ball Sleeve Travel.

APPENDIX B
CSMP PROGRAM

FLOW CHART



CSMP PROGRAM LISTING

INITIAL
 CONSTANT BM = 0.00015, JM = 0.001, P = 0.025, M = 1.0, ...
 A = 6.875, R = 1.987, KI = 15.9, ...
 KB = 0.112, LN = 6.6110
 PARAMETER TF = 0.0, JC = 0.30, JS2 = 0.0625, ...
 MH1 = 0.0, LS = 0.0016
 ES = 2.74, ITN = 0.0, ERROR = 0.001

*A DIMENSION OF ACTUATOR ARRANGEMENT IN
 *AM ANGULAR ACCELERATION OF THE MOTOR SHAFT RAD/SEC²
 *AO ANGULAR ACCELERATION OF THE OUTPUT FIN RAD/SEC²
 *A1 LS/RS -- THE INVERSE ELECTRICAL TIME CONSTANT
 *A2 JM/BM -- THE INVERSE MECHANICAL TIME CCNSTANT
 *BM COEFFICIENT OF VISCCUS FRICTION OZ-IN/RAD/SEC
 *DM ANGULAR DISPLACEMENT OF THE MOTOR SHAFT RAD
 *DO ANGULAR DISPLACEMENT OF THE FIN RAD
 *FOFTN FUNCTION OF NET TORQUE OF MOTCR OZ-IN
 *IS CURRENT GENERATED IN THE STATOR WINDINGS AMPERES
 *JC MOMENT OF INERTIA OF THE CRANK OZ-IN-SEC²
 *JM MOMENT OF INERTIA OF MOTOR SHAFT OZ-IN-SEC²
 *JS2 MOMENT OF INERTIA OF OUTPUT SHAFT OZ-IN-SEC²
 *KB BACK EMF CONSTANT VOLTS/(RAD/SEC)
 *KI TORQUE CONSTANT (OZ-IN)/AMPERE
 *L DISPLACEMENT OF BALL SCREW FROM MOTOR ANCHOR POINT IN
 *LS INDUCTANCE OF THE STATOR WINDINGS H
 *LN LINKAGE NULL; DISPLACEMENT OF BALL SCREW SUCH THAT
 * CRANK IS PERPENDICULAR TO MOTOR SHAFT IN
 *MH FIN HINGE MOMENT OZ-IN
 *M MASS OF THE BALL SCREW OZ
 *N GEAR RATIO
 *P PITCH IN/RAD
 *R DIMENSION OF ACTUATOR ARRANGEMENT IN
 *RS RESISTANCE OF 2 STATOR WINDINGS OHMS
 *TF SUM OF THE FRICTION FORCES ACTING ON THE BALL SCREW OZ-IN
 *TM TORQUE GENERATED BY MOTOR OZ-IN
 *TS1 TORQUE ACTING ON THE BALL SCREW DUE TO THE PRODUCT OF
 * MASS AND THE ACCELERATION OF THE BALL SCREW OZ-IN
 *VEMF BACK EMF VOLTS
 *VIN APPLIED VOLTAGE VOLT
 *VC ANGULAR VELOCITY OF THE FIN RAD/SEC
 *WM ANGULAR VELOCITY OF MOTOR SHAFT RAD/SEC
 *X LINEAR DISPLACEMENT OF THE BALL SCREW IN
 *X1 LINEAR VELOCITY OF THE BALL SCREW IN/SEC
 *X2 LINEAR ACCELERATION OF THE BALL SCREW IN/SEC²

NOSORT
 KE=KB/10.
 PI=2.0*ARSI(1.000000)
 A1 = LS / R;
 A2 = JM / B1
 THRST = 0.0
 JFAC = 0.0

*-----INTEGRATION METHOD-----
 METHOD RKSPX

DYNAMIC
 *-----MOTOR PROGRAM-----
 VIF= 30.0 * STEP(0.0)
 VIB = 0.0
 VIN = VIF + VIB
 VIN1 = VIN - VEMF
 ISSS = VIN1 * (1.0/RS)

```

*--CURRENT IS GENERATED IN AMPERES--
IS = REALPL(0.0,A1,ISSS)
*-----ACTUATOR PROGRAM-----
*--TM IS GENERATED IN OZ-IN--
TM = IS * KI
WM = INTGRL(0.0,AM)
DM = INTGRL(0.0,WM)
AO = AM / N
VO = WM / N
DO = DM / N
DO1 = COS(DO)
X2 = AM * P
X = DM * P
L = LN + X
DL = SQRT((2*A*R)**2 - (A**2 + R**2 - L**2)**2)
N = DL / (2*L*P)
TS1 = M * X2 * P
TC = JC * AJ * (1.0/(R*DO1)) * P
TO = JS2 * AO * (1.0/(R*DO1)) * P
TD = BM * W1
MH = MH1 * (1.0/(R*DO1)) * P
TL = TS1 + TC + TO + TF + TD + MH
TN2 = TN1 * (1.0/BM)
*--FOR COMPARISON WITH WM GENERATED THRU INTGRL AM--
WM1 = REALPL(0.0,A2,TN2)
*--CONVERSION FACTOR RAD/SEC TO RPM--
WMRPM = WM * (30./PI)
VEMF = WM * KB
VO DEG = VO * (180.0/PI)
DO DEG = DO * (180.0/PI)
*--COUNTS NUMBER OF ROTATIONS OF MOTOR SHAFT--
THCON = THRST
*--CONVERSION FACTOR (RAD/SEC)*OZ-IN TO WATTS--
PWR = WM * TM * .00706155

PROCEDURE TN1=FWD BWD(VIN,TM,TL)
TN1 = IMPL(ITN,ERRCR,FOFTN)
AM = TN1 / JM
IF(VIN.LT.0.0) GO TO 10
FOFIN = T1 - TL
GO TO 15
10 FOFIN = T1 + TL
15 CONTINUE
ENDPROCEDURE

PROCEDURE THRST=RESET(JFAC,DMDEG)
TS = JFAC * 360.0
THRST = DMDEG - TS
IF(THRST.LT.360.0) GO TO 40
JFAC = JFAC + 1.0
40 CONTINUE
ENDPROCEDURE

*--DEBUG PROCEDURE--
*OSORT
* CALL DEBUG(-5,0)

TERMINAL
TITLE BASIC EM ACTUATOR SYSTEM
TIME FINTI1 = .040
OUTPUT VODEG,DO DEG
* PRINT VODEG,DO DEG
LABEL MOTOR SPEED DUE TO STEP INPUT (30V)
PAGE MERGE

* PAGE XY PLOT
END
STOP
ENDJOB
/*

```

INITIAL DISTRIBUTION LIST

	No. copies
1. Commander, Naval Weapons Center Attn: R. F. Dettling, Code 3205 China Lake, CA 93055	5
2. Library, Code 0142 Naval Postgraduate School Monterey, CA 93943	4
3. Office of Research Administration Naval Postgraduate School Monterey, CA 93943	1
4. Professor R. H. Nunn, Code 69Nn Department of Mechanical Engineering Naval Postgraduate School Monterey, CA 93943	10

END

FILMED

2-85

DTIC